Dual symplectic classical circuits: An exactly solvable model of many-body chaos

Alexios Christopoulos[1*], Andrea De Luca[1], D L Kovrizhin [1], Tomaž Prosen [2]

1 Laboratoire de Physique Théorique et Modélisation, CY Cergy Paris Université, CNRS, F-95302 Cergy-Pontoise, France
2 Faculty of Mathematics and Physics, University of Ljubljana, Jadranska 19, SI-1000 Ljubljana, Slovenia
* alexios.christopoulos@cyu.fr

July 17, 2023

Abstract

We propose a general exact method of calculating dynamical correlation functions in dual symplectic brick-wall circuits in one dimension. These are deterministic classical many-body dynamical systems which can be interpreted in terms of symplectic dynamics in two orthogonal (time and space) directions. In close analogy with quantum dual-unitary circuits, we prove that two-point dynamical correlation functions are non-vanishing only along the edges of the light cones. The dynamical correlations are exactly computable in terms of a one-site Markov transfer operator, which is generally of infinite dimensionality. We test our theory in a specific family of dual-symplectic circuits, describing the dynamics of a classical Floquet spin chain. Remarkably, for these models, the rotational symmetry leads to a transfer operator with a block diagonal form in the basis of spherical harmonics. This allows us to obtain analytical prediction for simple local observables. We demonstrate the validity of our theory by comparison with Montecarlo simulations, displaying excellent agreement for different choices of observables.

Contents

1 Introduction

Symplectic dynamics is a powerful framework for understanding the behaviour of classical systems in a wide range of physical phenomena, from celestial mechanics to fluid dynamics. At its core, symplectic dynamics is concerned with the study of the evolution of systems that conserve phase space volume under Hamiltonian motion. This property is intimately related to the presence of a geometric structure known as a symplectic form, which encodes the essential dynamical information of the system. An example of this type of dynamics that has attracted a lot of interest is the classical spin chains. In particular, integrability has been studied for classical Heisenberg Spin Chain (CHSC) [1,2] in the $SU(2)$ symmetric case as well as in generalizations [3, 4] of it. Moreover, ergodicity has been studied for various types of 1D classical spin chain models [5–7] and the way it breaks [8] depending on the range of the interactions. Recently, the framework of fluctuating hydrodynamics [9], originally introduced in classical anharmonic chains, has been proven fruitful in the study of correlations [10–13] in classical ferromagnetic spin chains: in a suitable intermediate temperature regime, the system shows Kardar-Parisi-Zhang (KPZ) scaling. Quantum correspondence with spin chains [14] has demonstrated that there is good agreement in the high-temperature limit even when we are far away from the large spin $S \to \infty$ limit.

Dual symplectic dynamics is a quite novel idea according to which symplecticity characterizes both time and space propagation. It has been observed in $SO(3)$ invariant dynamics of classical spins [15], where the correlation function precisely follows KPZ class [10,16–18] and thus demonstrates spin transport with a dynamical exponent of $3/2$. More research has been done on the quantum analogue of dual symplecticity, which is dual unitarity in brickwall-type circuits. For this type of dynamics, the space and time propagators are both unitary. Interestingly, dual unitary quantum circuits can exhibit strongly chaotic quantum dynamics, whose classical simulation is in general expected to be exponentially hard in system size. Nonetheless, dual unitarity provides mathematical tools which lead to the exact calculation of certain dynamical quantities, such as spatiotemporal correlation functions [19–21], spectral Form Factor [22, 23], operator entanglement and entanglement growth [24, 25].

In this paper, we propose a general exact method of calculating dynamical correlations in dual symplectic brick-wall type 1D circuits. We show that similarly to what happens for dual-unitary quantum circuits, correlation functions in space and time over the equilibrium uniform measure of single-site observables $\langle O(x,t)O(0,0)\rangle$ is such that: i) they are non-vanishing only along light rays $x = \pm t$ (see below for details); ii) their behaviour on the light ray can be expressed as the matrix elements of a transfer operator. We demonstrate that our theory is in excellent agreement by comparison with a specific family of dual-symplectic spin chains, where local gates are composed of an Ising SWAP gate and one-site rotations. For this model, we prove that, despite the infinite dimensionality of the local phase space, the transfer operator involved in the calculation of the correlation function splits into finite-dimensional blocks, associated with the conservation of total angular momentum. Thanks to this decomposition, we obtain even analytic expressions for some observables and a simple and efficient numerical procedure for general ones. The paper is

organised as follows: in Section 2, we set up the general formalism for a symplectic system in a finite measure phase space; in Section 3, we focus on the dual symplectic case and by using a graphical representation, we obtain exact correlations for any local observables. In Section 4, we test our theory for the Ising SWAP model on a spin chain and explain the block-diagonal representation of the transfer operator using the conservation of the total angular momentum.

2 The model

We consider a classical dynamical system of N variables $\{\vec{X}_i\}$, with the site index $i = 0, \ldots, N-1$. For simplicity, we take N even. Also, we assume that each dynamical variable lives on the finite measure space M and the phase space of the whole system is obtained as the product of N copies, i.e. $M_N = M \times \ldots \times M$. The time is discrete $t \in \mathbb{Z}$ and interactions are local. In particular, we express the dynamics in terms of a local symplectic map acting on two sites only – the so-called (classical) gate, $\Phi : M \times M \to M \times M$. The dynamics of the whole system are then obtained acting with Φ on all pairs of neighbouring sites according to the brickwall circuit protocol and periodic boundary conditions $\vec{X}_{i+N} \equiv \vec{X}_i$ (see Fig. 1). More specifically, let's denote the local gate as $\Phi_{ij} : M_N \to M_N$ which acts as the map Φ on the variables $\vec{X}_i, \vec{X}_j$ and trivially with respect to all other variables. We can then introduce $\mathcal{T}_{even} = \Phi_{0,1}\Phi_{2,3} \ldots \Phi_{N-1,N}$ and similarly $\mathcal{T}_{odd} = \Sigma^{-1} \circ \mathcal{T}_{even} \circ \Sigma$, with the single-site translation $\Sigma : M_N \to M_N$, defined as $\Sigma(\vec{X}_0, \vec{X}_1, \ldots \vec{X}_{N-1}) = (\vec{X}_1, \ldots, \vec{X}_{N-1}, \vec{X}_0)$. From these two layers, we construct the *Floquet Operator* $\mathcal{T}$ that generate one period of the dynamics and takes the form:

$$\mathcal{T} = \mathcal{T}_{odd} \circ \mathcal{T}_{even} \tag{1}$$

By definition, it is true that $\Sigma^{-2}\mathcal{T}\Sigma^2 = \mathcal{T}$, meaning that there is a two-site translational invariance of the dynamics. We should also mention that for practical reasons we choose to represent a point of M_N with capital bold letters e.g $\boldsymbol{X} \equiv (\vec{X}_0, \vec{X}_1, \ldots \vec{X}_{N-1})$ whereas, a point of the single site space M is represented with a vector e.g $\vec{X}$.

It is useful to introduce a practical graphical notation. Specifically, we represent the local gate as a blue rectangle with two incoming and two outgoing legs

$\Phi =$ 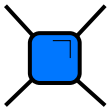 (2)

Each leg represents a copy of M and an operator has as many legs as the number of sites it acts on. With this in mind, the single-time step operator $\mathcal{T}$ is graphically depicted in Fig. 1.

The map Φ belongs to a specific group of transformations called the symplectic group. Symplecticity is a property appearing in Hamiltonian systems because they preserve the loop action [26]. In general, symplectic maps always involve d-pairs of conjugate variables, the configuration q and the momentum p, which can be seen as the coordinates of a $2d$ dimensional manifold $\mathcal{M}$ (phase space) endowed with the symplectic form ω [26] on $\mathcal{M}$. Then, a symplectic map $g : \mathcal{M} \to \mathcal{M}$, must satisfy $Dg^T \omega Dg = \omega$ for the Jacobian matrix Dg of the map g. Symplecticity automatically implies a unit determinant of the Jacobian $\det(Dg) = 1$ and thus conservation of the phase space volume. However, symplecticity is more restrictive than that and it actually, suggests that, the spectrum $\sigma(Dg) = \{g_i\}_{i=1}^{2d}$ of the Jacobian of the map includes only pairs of eigenvalues in the form $g_i, 1/g_i$. A

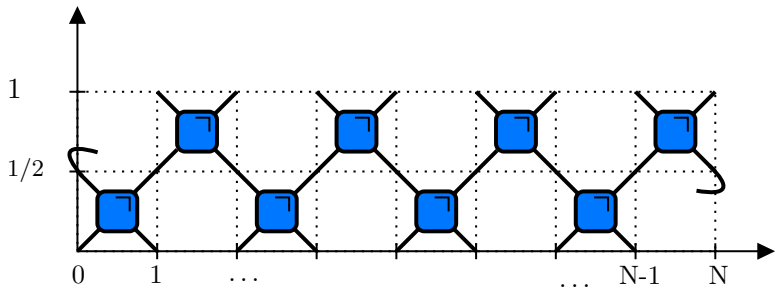

Figure 1: A graphical representation of the time evolution of a symplectic brick-wall circuit for a single period.

very important consequence of this property of $\sigma(Dg)$, is that the Lyapunov exponents $\lambda_i \quad i = 1, \ldots, 2d$ of the dynamics appear in pairs of $\pm\lambda_i$.

3 Dynamical correlations

3.1 Symplectic gate

In this section, we will consider 2-point correlation functions, and how the symplecticity of the dynamics can be used to simplify their calculation and draw some conclusions about their value. Before proceeding, we should establish some definitions. Firstly, we introduce the space of real functions over the phase space M_N

$$D(M_N) = \{\rho | \rho : M_N \to \mathbb{R}\} \tag{3}$$

An important role is played by phase-space distributions in $D(M_N)$ satisfying

$$\rho(\boldsymbol{X}) \in \mathbb{R}^+ , \qquad \int d\boldsymbol{X} \rho(\boldsymbol{X}) = 1 . \tag{4}$$

For technical reasons, it is however useful to consider the L^2 norm

$$\|\rho\|_2 = \left[\int d\boldsymbol{X} |\rho(\boldsymbol{X})|^2 \right]^{1/2} \tag{5}$$

and introduce the Hermitian product

$$\langle \rho_1 | \rho_2 \rangle = \int d\boldsymbol{X} \ \rho_1^*(\boldsymbol{X}) \rho_2(\boldsymbol{X}) , \qquad \rho_1, \rho_2 \in L^2(M_N) \tag{6}$$

with the braket notation $\langle \boldsymbol{X} | \rho \rangle = \rho(\boldsymbol{X})$. In general, any dynamical system with a map $h : M_N \to M_N$ on the phase space induces a dynamical transfer operator $\mathcal{P}_h : D(M_N) \to D(M_N)$. The map $\mathcal{P}_h$ is a linear operator known as Perron-Frobenius operator [27] with a Dirac delta kernel

$$\mathcal{P}_h(\boldsymbol{X}, \boldsymbol{Y}) = \delta\big(\boldsymbol{X} - h(\boldsymbol{Y})\big) , \quad \boldsymbol{X}, \boldsymbol{Y} \in M_N \tag{7}$$

and it performs the dynamics of a given density of initial conditions. In the case of the symplectic gate, which is invertible, the dynamical operator acts explicitly on a phase-space distribution ρ as :

$$(\mathcal{P}_\Phi \circ \rho)(\boldsymbol{X}) = \int_{M_2} d\boldsymbol{Y} \ \delta\big(\boldsymbol{X} - \Phi(\boldsymbol{Y})\big)\rho(\boldsymbol{Y}) = \rho\big(\Phi^{-1}(\boldsymbol{X})\big) , \quad \boldsymbol{X} \in M_2 \tag{8}$$

where we used the Jacobian of Φ being 1 since the map is invertible and volume preserving. The additional structure of the Hilbert space can be exploited to represent $\mathcal{P}_\Phi$ as an infinite dimensional unitary matrix. The unitarity $\langle\rho_1|\mathcal{P}_\Phi^\dagger\mathcal{P}_\Phi|\rho_2\rangle = \langle\rho_1|\rho_2\rangle$ follows from the volume preservation in phase space.

An important consequence of symplecticity, or in fact just volume conservation, is the invariance of the uniform (flat) measure on $L^2(M\times M)$ under the action of $\mathcal{P}_\Phi$. If we denote one site uniform measure as $u = 1/|M| \to |u\rangle$ with $|M|$ being the volume of the one site phase space M, then we can construct the 2-site uniform measure as $|u\rangle\otimes|u\rangle$. Then, symplecticity implies, based on (8), that any constant scalar is invariant under $\mathcal{P}_\Phi$ and thus the uniform density too, resulting in the following equations

$$\mathcal{P}_\Phi|u\rangle\otimes|u\rangle = |u\rangle\otimes|u\rangle\ , \qquad \langle u|\otimes\langle u|\mathcal{P}_\Phi = \langle u|\otimes\langle u| \tag{9}$$

where we use the fact that $\mathcal{P}_\Phi$ is a unitary operation in $L^2(M\times M)$ and thus the left and right eigenvectors are the same. It is convenient to work with the normalised state $|\circ\rangle = \|u\|_2^{-1}|u\rangle$ and choosing the graphical representation $|\circ\rangle =$ so Eq. (9) is graphically depicted as

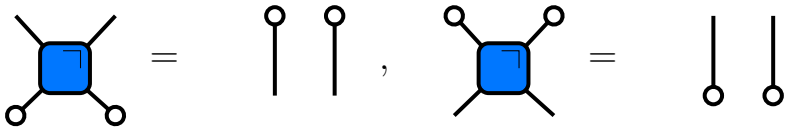

(10)

It is easy to check that this property implies that the stationary density of the Floquet transfer operator $\mathcal{T}$ is the uniform measure on M_N which is denoted as $|u_N\rangle = |u\rangle\otimes\ldots\otimes|u\rangle$. We also introduce the L^2–normalised version $|\circ_N\rangle = ||u_N||_2^{-1}|u_N\rangle$. Given any function on the phase space $a\in D(M_N)$, representing physical observable, we can express its average over the phase-space density ρ as

$$\int d\boldsymbol{X}\, a(\boldsymbol{X})\rho(\boldsymbol{X}) = \langle 1_N|\hat{a}|\rho\rangle \tag{11}$$

where the action of $\hat{a}$ is defined via $\langle\boldsymbol{X}|\hat{a}|\rho\rangle = a(\boldsymbol{X})\rho(\boldsymbol{X})$ and we make use of the unit scalar $|1_N\rangle \to 1_N(\boldsymbol{X}) = 1, \forall\boldsymbol{X}\in M_N$. Note that we have $|1\rangle = \sqrt{|M|}|\circ\rangle$. In general, for an ergodic symplectic system $|\circ_N\rangle$ is the unique invariant measure and thus at long times, any initial state will always converge to that. In our setting, we consider correlations of observables at large times and thus we focus on the invariant uniform measure. The connected dynamical correlation functions of one-site observables are defined as

$$C_{a,b}(i,j,t) \equiv \langle 1_N|\hat{b}_j\mathcal{T}^t\hat{a}_i|u_N\rangle - \langle b_j\rangle\langle a_i\rangle = \langle\circ_N|\hat{b}_j\mathcal{T}^t\hat{a}_i|\circ_N\rangle - \langle\circ_N|\hat{b}_j|\circ_N\rangle\langle\circ_N|\hat{a}_i|\circ_N\rangle \tag{12}$$

with $i,j = 0,\ldots,N-1$. In this expression, the local operators $\hat{a}_i$ act non-trivially only on the respective i-site meaning that they can be expressed as $\hat{a}_i = \mathbb{1}\otimes\cdots\otimes\overset{\text{site } i}{\hat{a}}\otimes\cdots\otimes\mathbb{1}$. The second term is just the product of the averages over the uniform measure which for a local observable is defined as $\langle a_i\rangle = \langle 1_N|\hat{a}_i|u_N\rangle = \langle\circ|\hat{a}|\circ\rangle$.

In the following, we focus mainly on the nontrivial first term $\langle 1_N|\hat{b}_j\mathcal{T}^t\hat{a}_i|u_N\rangle$ of the correlations, which can be graphically represented in Fig.2, where operations on one site such as $\hat{a}|\circ\rangle$ or $\hat{b}|\circ\rangle$ are indicated with a bullet $\bullet$. Moreover, using the two-shift invariance of the circuit one can always map the correlations from point i to 0 or 1 depending on the parity of i. This implies that the correlations split into two different types:

$$C_{a,b}(i,j,t) = \begin{cases} C^+_{a,b}(j-i,t) & i = even \\ C^-_{a,b}(j-i,t) & i = odd \end{cases} \tag{13}$$

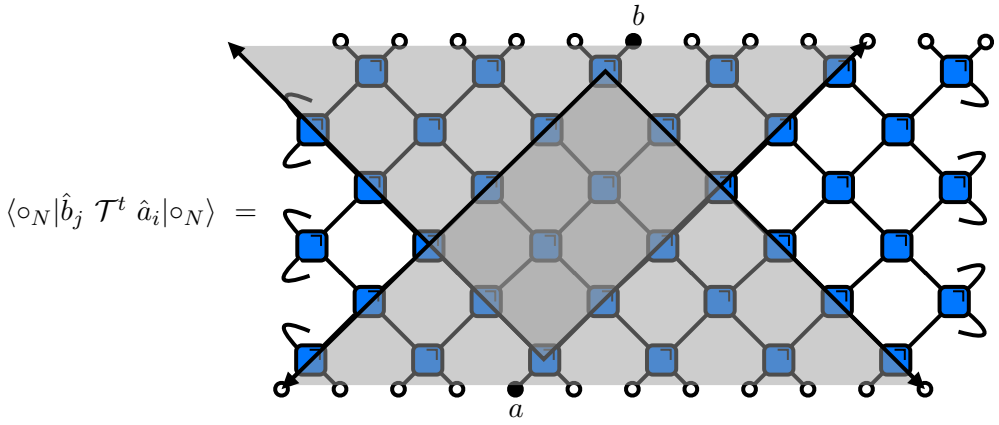

Figure 2: Graphical representations of the 2-point function. The shaded grey areas and the black arrows indicate the causal cones attached to each local observable. The symplecticity of Φ reduces this circuit to the cross-section (double-shaded area of the grid) of the causal cones.

As we can see in Fig. 2, by applying Eq. (10), we can erase all gates outside a light-cone spreading with velocity $v_c = 2$, from the position i of the operator $\hat{a}$ at the bottom. Similarly, we can argue from the top and the position j of the operator $\hat{b}$. This suggests that the only remaining gates must lie in the intersection between the forward and backward lightcones (see Fig. 2). In particular, when $|i-j| > 2t$ then these light cones are not overlapping with each other and the two observables are trivially uncorrelated. When $|i-j| \leq 2t$ the causal cones do overlap and can lead to non-trivially vanishing correlations. Additionally, for times $t > N/4$ the light cones reach the boundary: this introduces finite size effects to the correlations which makes the analytical calculations much more complicated. Here, we choose to focus on times $t \leq N/4$ where the correlation functions equal those computed in the thermodynamic limit $N \to \infty$. As explained above, we can make use of symplecticity of the gate $\mathcal{P}_\Phi$ as expressed by Eq. (10), to cancel all gates outside the intersection of the two lightcones. This leads to the following representation

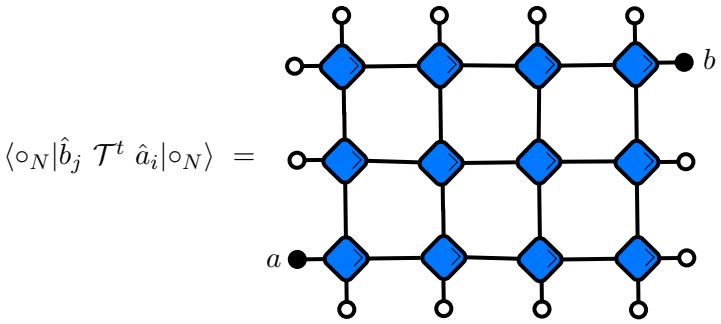

(14)

where the diagram is rotated by 45° and the local observables are not considered in general on the same edge of the light cone. The rectangle can be decomposed into rows or columns which, are represented as two different types of contracting transfer operators. This idea appears in the same manner in the folded picture of unitary circuits [19] and although it represents an important simplification, the calculation of 2-point correlation functions still remains challenging, in particular when $|i-j|$ does not scale with t, as the size of the involved transfer operators grows with time. We will see in the following section how for dual symplectic gates additional simplifications are possible leading to the explicit calculation of correlation functions.

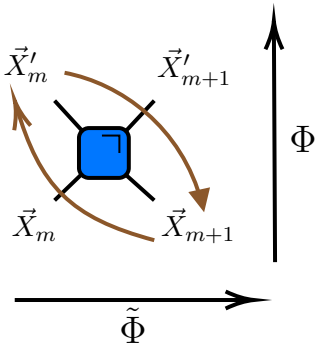

Figure 3: The local map Φ acting on two neighbouring spins and performing the temporal dynamics. By exchanging the diagonal legs we get its dual map $\tilde{\Phi}$ which performs the spatial dynamics. The diagonal exchange of the legs, exchanges the time and space axis leading to a map that propagates the temporal change in space.

3.2 Dual-symplectic gate

Here we add one more restriction to our dynamics. We demand that the local gate Φ is dual-symplectic meaning that the evolution of the system remains symplectic when one exchanges the roles of space and time. Specifically, the map performing the propagation in space is called dual map $\tilde{\Phi}$ and as in the dual-unitary case [24] it comes from the reshuffling of the diagonal legs as indicated in Fig. 3. This type of permutation of the legs leads to the exchange of time and space axis. In particular one can see from Fig.3 that in the dual picture, the two adjacent time moments of one site define the same time moments of its neighbouring site on the right. One can also say that for a dual symplectic system knowing the time evolution of one site, one can uniquely determine the time evolution of the whole system. In general, an arbitrary symplectic map typically has a dual-space propagator which is not unique (non-deterministic) or not even defined for all points in $M \times M$. Here we focus on a local gate Φ with a uniquely defined and symplectic $\tilde{\Phi}$. There has already been some research on dual symplectic integrable circuits and in particular in integrable circuits with non-abelian symmetries it has been demonstrated [15] that 2-point dynamical correlations follow Kardar–Parisi–Zhang (KPZ) universality.

With the additional property of dual symplecticity, the set of graphical contraction rules (10) are extended as:

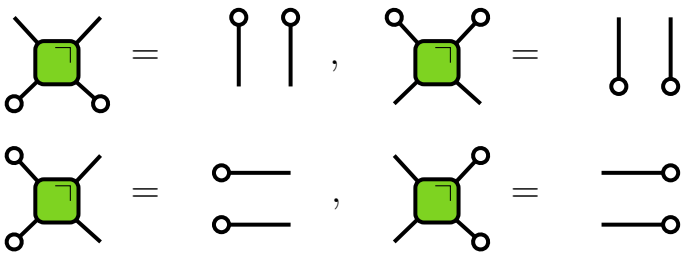

(15)

where the dual-symplectic gates are now being indicated with green colour. Dual symplecticity assures the invariance of the uniform measure in the space direction too. Its analogue in quantum systems is called dual unitarity and has been used to obtain exact results for a number of different systems [22, 28, 29]. There are similar expectations for dual- symplectic dynamics and indeed in the following, we show that one can find exactly the dynamic correlations and that they are non-vanishing only along the edges of the

causal cones with (13) becoming

$$C_{a,b}(i,j,t) = \begin{cases} \delta_{j-i,2t}\ C^{+}_{a,b}(2t,t) & i = even \\ \delta_{j-i,-2t}\ C^{-}_{a,b}(-2t,t) & i = odd \end{cases} \tag{16}$$

We are going to prove this using the diagrammatic representation established above. Specifically, one can simplify the correlations depicted in (14) by starting applying (15) at the edge of the rectangular area with neighbouring $|\circ\rangle$ states.

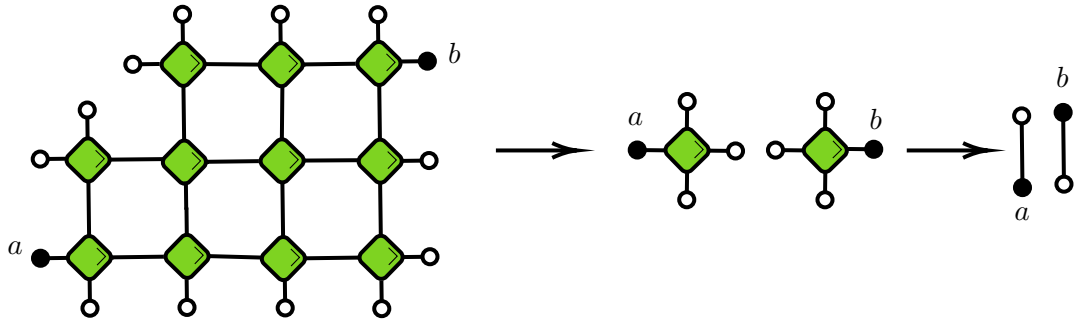

Repeating, this process we ultimately observe that the diagram trivialises to the second term of (12) and thus the connected correlations vanish. As long as this type of edge exists, the correlations will vanish except when the surface area of the cross-section is zero and the parities of the sites of the local observables are the same. This would practically imply that either of the sides of the cross-section has length zero and the rectangle reduces to just a line segment of length $2t$ with the local observables at the edges. From Fig. 2 one can see that depending on the parity of the site i there are two different types of line segments

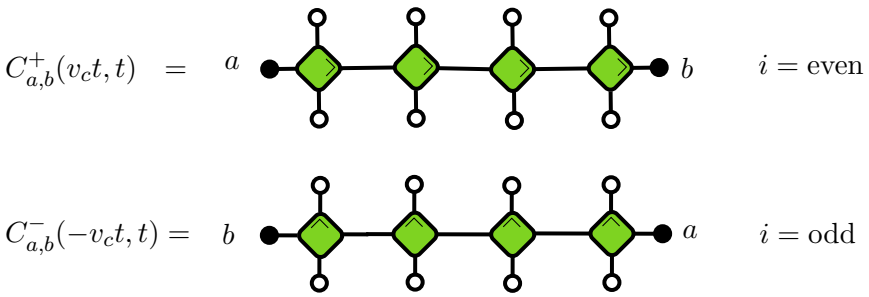

(17)

When i is even the correlation survives along the right-moving light edge and when i is odd it is the same for the left-moving one. Actually, one needs to study only one chirality of the correlations since the other can be obtained through a reflection of our circuit. As can be seen in Fig. 2, a reflection along the axis passing in between the points $(N/2-1, N/2)$ (which implies that every site $i = 0, \ldots, N-1$ is mapped to $N-1-i$), exchange the two edges of the causal-cone. Furthermore, this reflection does not change only the parity of the sites but also the order of the input and output states and thus the local gate is transformed as $\mathcal{P}_\Phi \to P \circ \mathcal{P}_\Phi \circ P$ where P is the swap operation.

The correlations in (17) can be expressed in terms of two different one-site transfer operators. In particular, we define the linear maps $\mathcal{F}_\pm : L^2(M) \to L^2(M)$ where $\pm$ corresponds to even, odd parity respectively. Graphically the transfer operators are represented in Fig. 4

Here one can also observe the reflection property mentioned above, which maps the transfer operator of one chirality to the other. For this reason, from now on we are going to

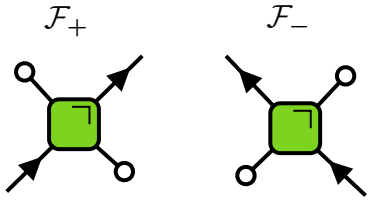

Figure 4: The graphical representation of the two different types of transfer operators $\mathcal{F}_\pm$. On the left (right) is the transfer operator appearing on the right (left) moving light edge on (17).

omit the label $\pm$ and focus only on the right moving light-edge with $\mathcal{F}_+ \equiv \mathcal{F}$. Afterwards, according to (17), the correlations along the edges of the light cone take the form:

$$C_{a,b}(2t,t) = \langle \circ | \hat{b}\, \mathcal{F}^{2t}\, \hat{a} | \circ \rangle - \langle \circ | \hat{b} | \circ \rangle \langle \circ | \hat{a} | \circ \rangle \tag{18}$$

This is an important exact result since it indicates that in dual-symplectic circuits the correlations are determined explicitly by transfer operators acting on a single site. The operator $\mathcal{F}$ is in general not Hermitian but, as proven in Appendix C, it is positive and weak contraction. Assuming that it has a pure point spectrum, as will be the case in the spin chain examples studied later, its spectral decomposition reads

$$\mathcal{F} = \sum_{i=0}^{\infty} \mu_i \, |\mu_i^R\rangle \, \langle \mu_i^L| \tag{19}$$

where we indicated the left and right eigenvectors as $|\mu_i^R\rangle, \langle \mu_i^L|$ and we ordered the eigenvalues as $|\mu_0| \geq |\mu_1| \geq \ldots$. As it is a weak contraction, its spectrum is on the unit disk, i.e. $|\mu_i| \leq 1$. We should also mention that as proved in [30] the eigenvalues lying with $|\mu_i| = 1$ have equal algebraic and geometric multiplicity, and thus their Jordan blocks are trivial. A direct consequence of the dual symplectic nature of $\mathcal{P}_\Phi$ is that the uniform measure is invariant under the action of $\mathcal{F}$. Therefore, the transfer operator always has the trivial eigenvalue $\mu_0 = 1$ with $|\mu_0^R\rangle = |\circ\rangle$ and $\langle \mu_0^L| = \langle \circ|$. Plugging the spectral decomposition (19) in Eq. (18),

$$C_{a,b}(v_c t, t) = \sum_{i=1}^{\infty} \langle \circ | \hat{b} | \mu_i^R \rangle \, \langle \mu_i^L | \hat{a} | \circ \rangle \, \mu_i^{2t} \tag{20}$$

where the $i = 0$ term in the sum is cancelled by the second term in Eq. (18). Note that the spectrum of $\mathcal{F}$ is related to the different levels of ergodicity of single-site observables. Depending on how many non-trivial eigenvalues are equal to 1 or have a unit modulus, dual symplectic circuits can demonstrate different levels of ergodicity. In particular, in the non-interacting case, all eigenvalues are unimodular with $|\mu_i| = 1$ and all correlations can either remain constant or oscillate around zero and in the non-ergodic case where more than one but not all eigenvalues are 1 correlations will decay to a non-thermal value. When the system is ergodic and non-mixing, all non-trivial μ_i are not 1 and at least one of them has unit modulus leading to correlations that oscillate around zero and thus their time averages vanish at large times. Finally, for an ergodic and mixing system, all μ_i are within the unit disk and all correlations decay to zero. A general example for the non-interacting case is the dual-symplectic local gate $\mathcal{P}_\Phi = P \circ (\mathcal{P}_{\phi_1} \otimes \mathcal{P}_{\phi_2})$ with P being the SWAP gate and ϕ_1, ϕ_2 being single site symplectic maps.

4 The Ising Swap model

Previously, we were studying an abstract dual-symplectic circuit. In order to test the previous analytical results, we choose to focus on a 1D classical spin chain where the local phase space is the unit sphere $M \equiv \mathcal{S}^2$. For this case, we choose to denote the coordinates $\vec{X}_i \equiv \vec{S}_i$ with the constraint $|\vec{S}_i| = 1$. We introduce the 3-parameter family of dual-symplectic local gates:

$$\Phi_{(\alpha,\beta,\gamma)} := \Big(R_x(\beta) \otimes R_x(\gamma)\Big) \circ I_\alpha \circ \Big(R_x(\gamma) \otimes R_x(\beta)\Big) \tag{21}$$

where the operation $R_\alpha(\theta), \theta \in [0, 2\pi)$ denotes a single spin rotation – SO(3) rotation matrix – around axis $\alpha \in \{x, y, z\}$ by the angle θ. We denote with I_α the SWAP Ising gate, whose action on a pair of sites reads

$$I_\alpha(\vec{S}_1, \vec{S}_2) = \big(R_z(\alpha S_1^z)\vec{S}_2, R_z(\alpha S_2^z)\vec{S}_1\big) \tag{22}$$

with α being the coupling constant of the interaction, $R_z(\theta)$ being a rotation around the z-axis and S_i^z being the z-component of $\vec{S}_i$. Assuming the standard Poisson bracket on the unit sphere

$$\{S_i^a, S_j^b\} = \delta_{ij}\epsilon_{abc}S_i^c \tag{23}$$

it is easy to recognize Eq. (22) as the symplectic evolution of two sites under the Hamiltonian $H_{12} = \alpha S_1^z S_2^z$ for a time $\delta t = 1$, followed by a SWAP operation $(S_1^a, S_2^a) \to (S_2^a, S_1^a)$.

It is easy to verify that the space-time dual of the gate (21), as defined in Fig. 3, has a similar form

$$\tilde{\Phi}_{(\alpha,\beta,\gamma)} \equiv (\mathbb{1} \otimes (-\mathbb{1})) \circ \Phi_{(\alpha,-\beta,\gamma)} \circ ((-\mathbb{1}) \otimes \mathbb{1}) \tag{24}$$

where we indicated by $\mathbb{1}$ the identity map and by $-\mathbb{1}$ the change of sign to all components $S_i^a \to -S_i^a$. Thus, the dual dynamics differ from the temporal ones by a simple sign-gauge transformation. As described in [15] our map $\Phi_{(\alpha,\beta,\gamma)}$ is called space-time self-dual since a flipping of the spins in a checker-board pattern leads to the recovery of the spatial dynamics from the temporal ones. Dual-symplectic circuits with local gates (21) enclose both ergodic and integrable cases depending on the choice of the parameters. For example, when $\alpha = 0$ the model becomes a trivial non-interacting one and thus integrability is expected. Another integrable case is when both β, γ take either of the values $0, \pi$ where the dynamics preserve the z-components of the spins along their respective light rays, leading to conserved extensive quantities along the parity's bipartition of the lattice. This type of local conserved quantities are called gliders and have already been studied in dual-unitary quantum circuits [31]. Having chosen our family of local gates, we proceed with the exact calculation of the correlations. As explained in the general formalism of Sec. 3.2, this requires the calculation of the transfer operators $\mathcal{F}$ acting on the single-site functions. In Appendix B we analytically find the transfer operator in both the phase space and the density space:

$$f = R_x(\gamma)Q(\alpha)R_x(\gamma) \quad , \quad \mathcal{F} \equiv \mathcal{P}_f \tag{25}$$

with $Q(\alpha) = \frac{1}{2}\int_{-1}^{1} dz' R_z(\alpha z')$ and $f : M \to M$. The transfer operator is just the Perron–Frobenius of f and its kernel is given in the same way as in (7) for a single site phase space. It is interesting to note that (25) is completely independent of β. The other chirality of the correlation is simply recovered from the middle point reflection $P \circ \mathcal{P}_{\Phi_{\alpha,\beta,\gamma}} \circ P = \mathcal{P}_{\Phi_{\alpha,\gamma,\beta}}$ which is equivalent with just changing $\beta, \gamma \to \gamma, \beta$. The fact that (25) is expressed in terms of rotations suggests the use of spherical harmonics as a convenient basis for the L^2 density space. We choose the coordinates z, φ being respectively the z cartesian component and the azimuthal angle. Then, the spherical harmonics

$|\ell, m\rangle \to Y_{\ell,m}(z,\varphi)$ for $\ell = 0, 1, \ldots$ and $|m| \leq \ell$ form a suitable orthonormal basis for L^2 functions. Our approach is based on finding the representation of the transfer operator in this basis. As we rigorously prove in Appendix B, the transfer operator $\mathcal{F}$ preserves the total angular momentum and thus has a block diagonal form in ℓ, with each block having dimension $2\ell+1$. It follows that the eigenvectors and eigenvalues in Eq. (19) can be indexed by a block index ℓ and an index $\tilde{m}$ within each block. Thus, Eq. (20) takes the form

$$C_{a,b}(2t,t) = \sum_{\ell=1}^{\infty} \sum_{\tilde{m}=-\ell}^{\ell} \langle \circ|\hat{b}|\mu^R_{\ell,\tilde{m}}\rangle \, \langle \mu^L_{\ell,\tilde{m}}|\hat{a}|\circ\rangle \, \mu^{2t}_{\ell,\tilde{m}} \tag{26}$$

From this expression, it follows that if the local observables $|a_x\rangle, |b_y\rangle$ expand only over a finite number of total angular momentum subspaces, then the sum in Eq. (26) only contains a finite number of terms; in particular only the common values of ℓ between the two observables will matter. For example, the observable $a(z,\phi) = z^2$ has non-vanishing overlaps only for $\ell = 0, 2$. Similarly, any polynomial in the variable z only involves a finite number of blocks. This is an important property of our system, proved in Appendix D, since it suggests that a finite set of exponentials (in t) fully capture the behaviour of the 2-point correlations whenever one of the two observables a, b involves only a finite number of ℓ blocks. In practice, one can calculate the exact dynamical correlations just by diagonalizing the relevant finite-dimensional blocks of $\mathcal{F}$. Moreover, observables which have no overlapping such subspaces lead to vanishing correlations for every t.

At this point, we provide some analytic results for the choice of $a(z,\phi) = z^n$, $b(z,\phi) = z$ with $n \in \mathbb{Z}^+$. In this case a has non vanishing overlaps for $\ell = 0, 2, \ldots n$ if n even and $\ell = 1, 3, \ldots n$ if n odd and b for $\ell = 1$. We can see that for the case of n even there are no common overlapping subspaces between the two observables and thus the correlations vanish for all t. However, when n is odd, the correlations depend only on the $\ell = 1$ block of $\mathcal{F}$ and by using (25) one can explicitly find that the eigenvalues of this block are :

$$\begin{aligned} \mu_{1,0} &= \frac{\sin(\alpha)}{\alpha} \\ \mu_{1,-1} &= \frac{(\alpha + \sin(\alpha))\cos(2\gamma) - \Delta(\alpha,\gamma)}{2\alpha} \\ \mu_{1,1} &= \frac{(\alpha + \sin(\alpha))\cos(2\gamma) + \Delta(\alpha,\gamma)}{2\alpha} \end{aligned} \tag{27}$$

where $\Delta(\alpha,\gamma) = \sqrt{(\alpha+\sin\alpha)^2\cos^2(2\gamma) - 4\alpha\sin(\alpha)}$. Since only the $\ell = 1$ subspace contributes, we only need the overlaps of the observables with this subspace :

$$\langle 1m|z^n\rangle = \frac{2\sqrt{3\pi}}{n+2}\delta_{m,0} \tag{28}$$

The observable z^n does not depend on the azimuthal angle and thus it depends only on the spherical harmonics $|\ell m\rangle$ with $m = 0$. By diagonalizing the block of $\mathcal{F}$ that corresponds to $\ell = 1$ and using (27),(28) one can recover the exact expression for the correlations:

$$\begin{aligned} C_{a,b}\,(2t,t) &= \frac{1}{2^{2t+1}(n+2)}\left(\mathcal{E}^+(t) + \mathcal{E}^-(t)\right) \\ \mathcal{E}^{\pm}(t) &= \left(1 \pm \frac{\alpha - \sin\alpha}{\Delta}\right)\left(\frac{(\alpha+\sin\alpha)\cos(2\gamma) \pm \Delta}{\alpha}\right)^{2t} \end{aligned} \tag{29}$$

where the other chirality is recovered with just $\gamma \to \beta$. In the special integrable cases, one finds:

$$\lim_{\alpha\to 0} C_{a,b}\,(2t,t) = \frac{\cos(4\gamma t)}{2+n} \quad , \quad \lim_{\gamma\to 0} C_{a,b}\,(2t,t) = \frac{1}{2+n} \tag{30}$$

In Fig. 5 we demonstrate numerically that the correlations survive only along the edges of the causal cone and verify (29) in the case of $n = 1$. Here it is important to mention that we consider the symmetries of our circuit for the estimation of the correlations. In particular, except the 2-site translation invariance there is also a 1 time step translation invariance because the correlations are evaluated over the invariant measure and both of these symmetries allow us to perform averaging over a larger sample size and obtain more accuracy for the numerical data.

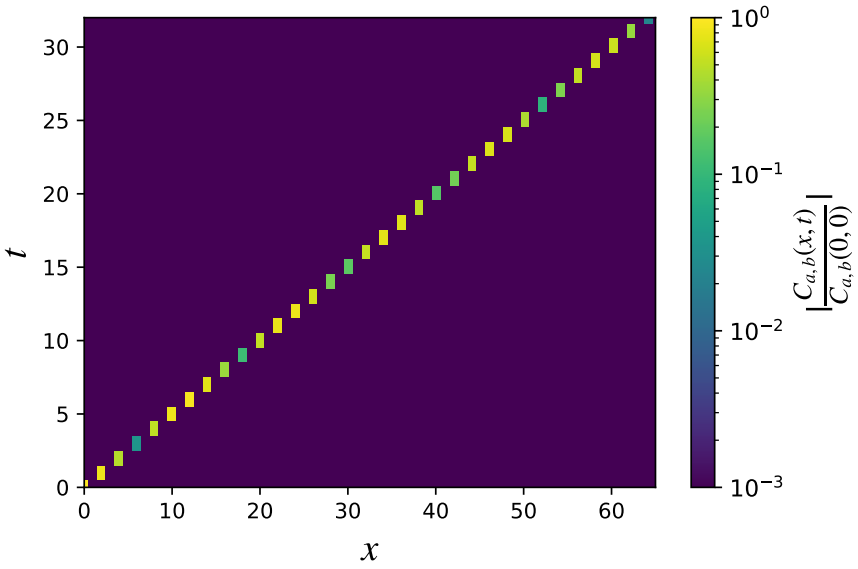

(a)

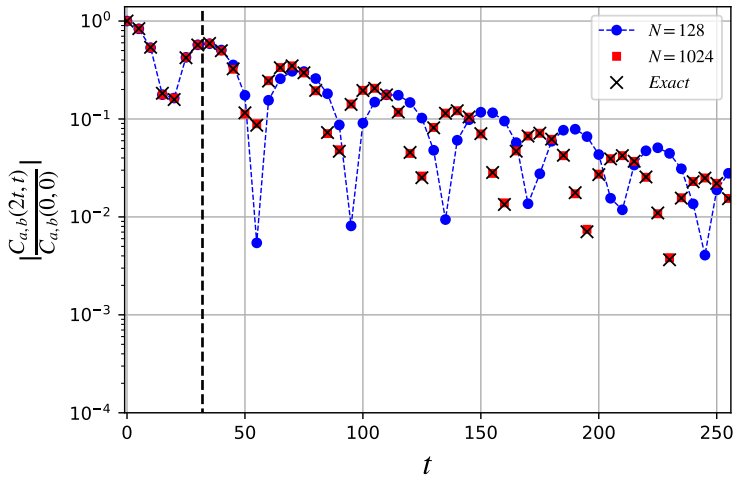

(b)

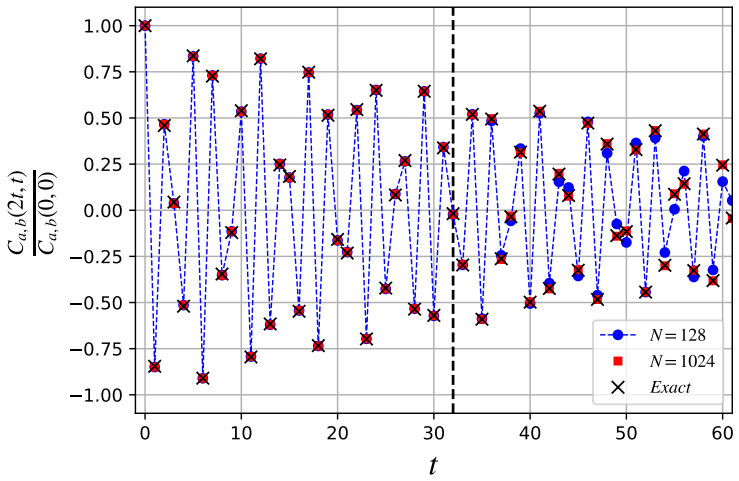

(c)

Figure 5: Auto-correlations for the S^z spin component, normalized by the maximum value $C_{a,b}(0,0)$ for system of sizes $N = 128, 1024$ spins with the parameters being $\alpha = 0.3$ and $\beta = \frac{\sqrt{2}}{4}\pi, \gamma = \frac{\sqrt{2}}{2}\pi$ and with a sampling size of $N_{sample} = 50000$ for the initial conditions. (a): The spatiotemporal correlator $|C_{a,b}(x,t)/C_{a,b}(0,0)|$ in the case of $N = 128$ where we can observe that it vanishes off the edge ($x = v_c t$) of the causal cone. (b): The comparison of $|C_{a,b}(x,t)/C_{a,b}(0,0)|$ on the right edge of the causal cone with the theoretical result obtained through (29) with exact diagonalization of $\mathcal{F}$ at $\ell = 1$ subspace. The numerical results are obtained for two different sizes $N = 128, 1024$ and plotted with a time step of 5 in a log scale. The dashed line represents the time moment $t = N/4$ for the system $N = 128$ when it stops being in the effective thermodynamic limit and our theory is invalid. The system $N = 128$ stops agreeing with the exact result after this time moment, but the larger system $N = 1024$ still demonstrates excellent agreement with the theory. (c): The comparison of $C_{a,b}(x,t)/C_{a,b}(0,0)$ on the right edge of the causal cone but with a linear scale for the vertical axis.

5 Conclusion

We have provided an exact way of calculating dynamic correlations in dual-symplectic classical circuits, where we also proved that the correlations are non-vanishing only along the edges of the light cones and completely specified in terms of a weakly contracting, positive one-site transfer operator. It is important to mention that our method is valid not only for dual-symplectic systems. Specifically, it is easy to check that any local gate Φ which is volume preserving that also has a volume-preserving dual map $\tilde{\Phi}$, satisfy (15) and thus exhibit the same diagrammatic behaviour. Every symplectic map is volume and orientation-preserving, but the group of symplectic diffeomorphisms is significantly smaller than that of the volume-preserving ones (Non-squeezing theorem [32]). Consequently, there is a larger set of dynamical ergodic systems that exhibit our diagrammatic representation with correlations that vanish everywhere except on the edges of the light cone. In addition, we prove that for the relevant case of the Ising SWAP model, the transfer operator exhibits a block-diagonal form which leads to an expansion involving only the common ℓ subspaces of the observables. This property has the great advantage of no need

for truncation and recovery of analytical results through exact diagonalization with each (finite) block.

We close with some naturally arising questions. Is it possible to find a more general characterization or complete parametrization of the dual symplectic circuits which may help in also finding a parametrization of dual unitary gates [30] to larger than qubits local spaces? Could one find exact results for other initial densities as has already been demonstrated in the dual unitary case [29]? Our formalism can be a stepping stone to studying these types of questions for the novel class of dual-symplectic systems.

Acknowledgements

T.P acknowledges financial support from Program P1-0402, and Grants N1-0219 and N1-0233 of the Slovenian Research and Innovation Agency (ARIS). D.K acknowledges partial support from Labex MME-DII (Modèles Mathématiques et Economiques de la Dynamique, de l'Incertitude et des Interactions), ANR11-LBX-0023 and LPTM ANR INEX 2020 EMERGENCE CMTNEQ grants. A. D. L. acknowledges support by the ANR JCJC Grant ANR-21- CE47-0003 (TamEnt). A.C acknowledges support from the EUTOPIA PhD Co-tutelle program.

A Representation of $\mathcal{P}_{\Phi_{(\alpha,\beta,\gamma)}}$ in spherical harmonics

Here we analytically find the matrix elements of the Perron-Frobenius operator $\mathcal{P}_{\Phi_{(\alpha,\beta,\gamma)}}$ of the local gate in the basis of spherical harmonics. We denote this basis as $|\ell, m\rangle \rightarrow Y_{\ell,m} \quad \ell = 0, \ldots, \infty \quad , |m| \leq \ell$ and is clearly orthonormal with respect to the inner product (6):

$$\langle \ell_1 m_1 | \ell_2 m_2 \rangle = \int_{\mathcal{S}^2} d\vec{X} \; Y^*_{\ell_1 m_1}(\vec{X}) Y_{\ell_2 m_2}(\vec{X}) = \delta_{\ell_1,\ell_2}\delta_{m_1,m_2} \tag{A.1}$$

As follows from (21) the local gate is composed of local one site rotations $R_x(\theta) \quad \theta \in [0, 2\pi)$ and the Ising SWAP gate I_α. The rotations around the x-axis are trivially known in the basis of spherical harmonics as $\mathcal{P}_{R_x(\theta)} = D(-\pi/2, \theta, \pi/2)$ where D is the Wigner-D matrix [33] and is block diagonal in ℓ ($\langle \ell_1 m_1 | D | \ell_2 m_2 \rangle = 0$ when $\ell_1 \neq \ell_2$) with the right choice of Euler angles. Thus, we need only to find the representation of I_α. Our approach is based on firstly finding the kernel of the Ising gate on $\mathcal{S}^2 \times \mathcal{S}^2$ and then using that result to finally obtain its representation on $|\ell, m\rangle$.

We already know from (22) how I_α acts on two spins and this leads to the following Kernel:

$$\mathcal{P}_{I_\alpha}(\vec{X}_1, \vec{X}_2, \vec{X}_3, \vec{X}_4) = \delta\big(\vec{X}_1 - R_z(\alpha z_3)\vec{X}_4\big) \; \delta\big(\vec{X}_2 - R_z(\alpha z_4)\vec{X}_3\big) \tag{A.2}$$

we should mention here that we choose the polar coordinates $\vec{X}_i = (z_i, \varphi_i) \quad i = 1, \ldots, 4$ for the parametrization of the unit sphere. This operation couples two spins and thus by using (6) in the basis of two-spherical harmonics we obtain:

$$\begin{aligned}\langle \ell_1 m_1, \ell_2 m_2 | \mathcal{P}_{I_\alpha} | \ell_3 m_3, \ell_4 m_4 \rangle = \; & \delta_{m_1,m_4}\delta_{m_2,m_3} \\ & \int_{\mathcal{S}^2} d\vec{X}_3 d\vec{X}_4 \; Y^*_{\ell_1 m_1}(R_z(\alpha z_3)\vec{X}_4) Y_{\ell_4 m_4}(\vec{X}_4) \; Y^*_{\ell_2 m_2}(R_z(\alpha z_4)\vec{X}_3) Y_{\ell_3 m_3}(\vec{X}_3)\end{aligned} \tag{A.3}$$

The Kronecker deltas come from performing the integration over φ_3, φ_4 and in the expression above we can see the coupling of the rotations with the z-component of each other's vector. To continue our calculation we have to mention that a rotation around the z-axis is

just a translation over the azimuthal angle and due to that the spherical harmonics satisfy $Y_{\ell,m}(R_z(\theta)\vec{X}) = Y_{\ell,m}(\vec{x})e^{im\theta}$. Based on this property one can decouple the z-components as:

$$\langle \ell_1 m_1, \ell_2 m_2 | \mathcal{P}_{I_\alpha} | \ell_3 m_3, \ell_4 m_4 \rangle = \int_{\mathcal{S}^2} d\vec{X}_3 d\vec{X}_4 \; Y^*_{\ell_1 m_1}(R_z(\alpha \frac{m_2}{m_1} z_4)\vec{X}_4) Y_{\ell_4 m_4}(\vec{X}_4) \; Y^*_{\ell_2 m_2}(R_z(\alpha \frac{m_1}{m_2} z_3)\vec{X}_3) Y_{\ell_3 m_3}(\vec{X}_3) \quad \text{(A.4)}$$

At this point, we manage to couple the rotations R_z of one spin with its own z- component. This type of nonlinear rotation is called 'torsion' $T(a)\vec{X} = R_z(az)\vec{X}$ (where a is the coupling constant with $T(0) = \mathbb{1}$) and its representation in spherical harmonics has been calculated in [34]. In particular, it was found that:

$$\langle \ell m | T(a) | \ell' m' \rangle \;=\; \delta_{m,m'}(-1)^m \sqrt{(2\ell+1)\,(2\ell'+1)} \sum_{p=|\ell-\ell'|}^{\ell+\ell'} (-i)^p j_p(-ma) C^{\ell\ell' p}_{000} C^{\ell\ell' p}_{-mm0}. \quad \text{(A.5)}$$

where j_p is the spherical Bessel function and $C^{\ell_1,\ell_2,\ell_3}_{m_1,m_2,m_3}$ are the Clebsch-Gordan coefficients. Finally, we recover the representation of the Ising SWAP gate:

$$\langle \ell_1 m_1, \ell_2 m_2 | \mathcal{P}_{I_\alpha} | \ell_3 m_3, \ell_4 m_4 \rangle = \langle \ell_1 m_1 | T(\alpha \frac{m_2}{m_1}) | \ell_4 m_1 \rangle \; \langle \ell_2 m_2 | T(\alpha \frac{m_1}{m_2}) | \ell_3 m_3 \rangle \; \delta_{m_1,m_4} \delta_{m_2,m_3} \quad \text{(A.6)}$$

This expression is valid even when $m_1, m_2 = 0$ since as we can observe from (A.5) that the denominators cancel out in the argument of j_p. Now, we only need to combine all the above and find out that the representation of the local gate of the dynamics is:

$$\langle \ell_1 m_1, \ell_2 m_2 | \Phi_{\alpha,\beta,\gamma} | \ell_3 m_3, \ell_4 m_4 \rangle = \sum_{q_1,q_2=-\ell_1,-\ell_2}^{\ell_1,\ell_2} \langle \ell_1 m_1 | \mathcal{P}_{R_x(\beta)} | \ell_1 q_1 \rangle \langle \ell_4 q_1 | \mathcal{P}_{R_x(\beta)} | \ell_4 m_4 \rangle \langle \ell_2 m_2 | \mathcal{P}_{R_x(\gamma)} | \ell_2 q_2 \rangle \langle \ell_3 q_2 | \mathcal{P}_{R_x(\gamma)} | \ell_3 m_3 \rangle \times$$
$$\times \langle \ell_1 q_1 | T(\alpha \frac{q_2}{q_1}) | \ell_4 q_1 \rangle \; \langle \ell_2 q_2 | T(\alpha \frac{q_1}{q_2}) | \ell_3 q_2 \rangle \quad \text{(A.7)}$$

B Block Diagonal form of $\mathcal{F}_\pm$

In this appendix, we analytically calculate the matrix of the one-site transfer operator in the spherical harmonics representation and prove that it has a block diagonal form in ℓ. Our calculation is based on the direct interpretation of Fig. 4. In particular, for a general local gate, one can interpret $\mathcal{F}_\pm$ either in the time direction where the dynamics are performed by Φ, or in the space one where we can use the dual picture with $\tilde{\Phi}$. Both of these pictures are equivalent but here we choose the former one. Like in the main text we choose to focus on the right-moving chirality $\mathcal{F}_+ \equiv \mathcal{F}$ and omit the $\pm$ label. According to this choice, one can see from Fig. 4 that the transition amplitudes of $\mathcal{F}$ for two arbitrary densities (functions) ρ_1, ρ_2 from $L^2(M)$ are:

$$\langle \rho_1 | \mathcal{F} | \rho_2 \rangle = (\langle \circ | \otimes \langle \rho_1 |) \; \mathcal{P}_\Phi \; (|\rho_2\rangle \otimes |\circ\rangle) \quad \text{(B.1)}$$

This is true for any dual-symplectic gate. We focus on the Ising swap model where since $|\circ\rangle = |00\rangle$ in the basis spherical harmonics one can directly use (B.1),(A.6),(A.7) to obtain:

$$\langle \ell m|\mathcal{F}|\ell' m'\rangle = \langle 00, \ell m|\mathcal{P}_{\Phi_{\alpha,\beta,\gamma}}|\ell' m', 00\rangle = \delta_{\ell,\ell'} \sum_{q_2=-\ell}^{\ell} \langle \ell m|\mathcal{P}_{R_x(\gamma)}|\ell q_2\rangle \frac{\sin(\alpha q_2)}{a q_2} \langle \ell q_2|\mathcal{P}_{R_x(\gamma)}|\ell m'\rangle \tag{B.2}$$

where we used that $T(0) = \mathbb{1}$, $C^{0,0,0}_{0,0,0} = 1$ and $j_0(x) = \sin(x)/x$. Moreover, we used that a constant scalar is invariant under rotations and thus $\langle 00|\mathcal{P}_{R_x(\beta)}|00\rangle = 1$. This expression can be compactified even more by defining the map $Q(\alpha) : M \to M$

$$Q(\alpha) = \frac{1}{2}\int_{-1}^{1} dz' R_z(\alpha z') \tag{B.3}$$

The spherical harmonics are the eigenbasis of the Perron-Frobenius operator of rotations around the $z-$axis and in particular $\langle \ell_1 m_1|\mathcal{P}_{R_z(\theta)}|\ell_2 m_2\rangle = e^{-i m_1 \theta}\delta_{\ell_1,\ell_2}\delta_{m_1,m_2}$ for a rotation of an angle $\theta \in [0, 2\pi)$. Then, using this in (B.3) and performing the integration one recovers the representation of $\mathcal{P}_{Q(\alpha)} : D(M) \to D(M)$.

$$\langle \ell_1 m_1|\mathcal{P}_{Q(\alpha)}|\ell_2 m_2\rangle = \frac{\sin(\alpha m_1)}{\alpha m_1}\ \delta_{\ell_1,\ell_2}\delta_{m_1,m_2} \tag{B.4}$$

we finally recover the exact form of the transfer operator:

$$\mathcal{F} = \mathcal{P}_{R_x(\gamma)}\mathcal{P}_{Q(\alpha)}\mathcal{P}_{R_x(\gamma)} \tag{B.5}$$

and this automatically implies that the latter is just the Perron-Frobenius operator of the local phase-space map $f : M \to M$:

$$f = R_x(\gamma)Q(\alpha)R_x(\gamma) \quad , \quad \mathcal{F} \equiv \mathcal{P}_f \tag{B.6}$$

We managed to find the exact form of the transfer operator in both the density space and pointwise map in phase space and as we can see in (B.2), it is block diagonal in the total angular momentum ℓ and thus preserves it. This is not surprising, since as we can see from (B.3),(B.6) the transfer operator is just a composition of rotations, which preserve the total angular momentum. The results for $\mathcal{F}_-$ can be recovered from the above with the use of the middle point reflection $\beta, \gamma \to \gamma, \beta$.

C Weak contractivity and positivity of $\mathcal{F}_\pm$

In this appendix, we are proving explicitly that the single-site transfer operator $\mathcal{F}$ ($\equiv \mathcal{F}_+$) is a weak contraction as well as a positive operator. Firstly, as mentioned in the main text, the map $\mathcal{P}_\Phi$ is unitary in $L^2(M \times M)$ since it preserves the L^2-norm. Then according to this from (B.1) we can obtain for every $\rho_1, \rho_2 \in L^2(M)$:

$$\begin{aligned} |\langle \rho_1|\mathcal{F}|\rho_2\rangle| = |(\langle \circ| \otimes \langle \rho_1|)\ \mathcal{P}_\Phi\ (|\rho_2\rangle \otimes |\circ\rangle)| &\leq \|\ |\circ\rangle \otimes |\rho_1\rangle\|_2\ \|\mathcal{P}_\Phi\ (|\rho_2\rangle \otimes |\circ\rangle)\|_2 \\ &= \|\ |\circ\rangle \otimes |\rho_1\rangle\|_2\ \|\ |\rho_2\rangle \otimes |\circ\rangle\|_2 = \|\rho_1\|_2\ \|\rho_2\|_2 \end{aligned} \tag{C.1}$$

where we used the Cauchy–Schwarz inequality and the fact that the state $|\circ\rangle$ is normalised. Now by setting $|\rho_1\rangle = \mathcal{F}|\rho_2\rangle$ one recovers:

$$\|\mathcal{F}|\rho_2\rangle\|_2 \leq \|\rho_2\|_2 \tag{C.2}$$

for every $\rho_2 \in L^2(M)$. This suggests that the single-site transfer operator is a weak contraction.

The positivity is a direct consequence of the properties of the Perron-Frobenius operator. In particular, let us assume that $\rho \in L^2(M)$ and $\vec{X} \in M$ then we are interested in the value of the scalar $\langle \vec{X}|\mathcal{F}|\rho\rangle$. It is sufficient to prove that this is always positive if $\rho \geq 0$. The calculation is based on using (B.1) from which we get:

$$\langle \vec{X}|\mathcal{F}|\rho\rangle = \left(\langle \circ| \otimes \langle \vec{X}|\right)\, \mathcal{P}_\Phi\, \left(|\rho\rangle \otimes |\circ\rangle\right) \tag{C.3}$$

The scalar $|\circ\rangle \to u_\circ(\vec{X}) = 1/\sqrt{|M|}$ is positive, thus if we assume $\rho \geq 0$ then $|\rho\rangle \otimes |\circ\rangle \to (\rho u_\circ)(\vec{X}_1, \vec{X}_2) = \rho(\vec{X}_1)u_\circ(\vec{X}_2)$ is a non-negative scalar too. Now, as the last step we need to mention that, the local operation $\mathcal{P}_\Phi$ is a Frobenius-Perron operator, which by definition is positive and thus implies that $\mathcal{P}_\Phi\, (|\rho\rangle \otimes |\circ\rangle \geq 0$. Then, as a consequence the value (C.3) is non negative for every $\vec{X} \in M$ meaning that:

$$\mathcal{F}|\rho\rangle \geq 0 \quad \text{for any } \rho \geq 0 \in L^2(M)$$

In the same way, one can prove these properties for $\mathcal{F}_-$ too.

D Contributing modes to the correlations

In this section we prove that the only contributing ℓ-subspaces to the correlations are the common ones of the expansions of the observables over the spherical harmonics. We denote these subspaces as $V^\ell = span(\{|\ell, m\rangle\}_{m=-\ell}^{\ell})$. The proof is a consequence of the block diagonal form of $\mathcal{F}$ ($\equiv \mathcal{F}_+$). Specifically, the transfer operator is block diagonal in ℓ meaning that it is just the direct sum $\mathcal{F} = \overset{\infty}{\underset{\ell=0}{\oplus}} \mathcal{F}^\ell$, where $\mathcal{F}^\ell$ are the blocks of each total angular momentum subspace. It is thus, convenient to work in the picture where the Hilbert space $L^2(\mathcal{S}^2) = \overset{\infty}{\underset{\ell=0}{\oplus}} V^\ell$ is a direct sum of the total angular momentum subspaces. Now according to this picture, the two local observables mentioned in the main text would also be decomposed as $|a\rangle = \overset{\infty}{\underset{\ell=0}{\oplus}} |a^\ell\rangle \quad , |b\rangle = \overset{\infty}{\underset{\ell=0}{\oplus}} |b^\ell\rangle$. Assume that their expansions over the spherical harmonics overlap only with a finite number of V^ℓ spaces which we denote as $\ell_i^a \quad i = 1, \ldots, n_a$ and $\ell_j^b, \quad j = 1, \ldots, n_b$ respectively. The integers n_a, n_b are the total number of overlapping V^ℓ of the observables. This would imply that the components $|a^\ell\rangle, |b^\ell\rangle$ vanish trivially at the rest of the total angular momentum subspaces:

$$\begin{aligned} |a^\ell\rangle &= \vec{0}_\ell \text{ for } \ell \neq \ell_i^a \\ |b^\ell\rangle &= \vec{0}_\ell \text{ for } \ell \neq \ell_j^b \end{aligned} \tag{D.1}$$

where $\vec{0}_\ell$ is the zero vector in V^ℓ. Moreover, in this picture, the Hermitian product breaks into a sum of Hermitian products over V^ℓ and by using $|\circ\rangle = |1\rangle/2\sqrt{\pi}$ we obtain from (18)

$$C_{a,b}(t,t) = \frac{1}{4\pi}\Big(\sum_{\ell=0}^{\infty}\langle a^\ell|(\mathcal{F}^\ell)^{2t}|b^\ell\rangle - \frac{1}{4\pi}\langle 1|b\rangle\langle 1|a\rangle\Big) = \frac{1}{4\pi}\sum_{\ell_c\neq 0}\langle a^{\ell_c}|(\mathcal{F}^{\ell_c})^{2t}|b^{\ell_c}\rangle \tag{D.2}$$

where we applied (D.1) and now one can observe that the only non-vanishing terms are the ones of the common subspaces ℓ_c between ℓ_i^a and ℓ_j^b. The space V^0 of the constant on $\mathcal{S}^2$ scalars do not contribute to the correlations since it is being cancelled out from the second term in (D.2). In addition, our result automatically implies that only the eigenvalues of $\mathcal{F}^{\ell_c}$ contribute and thus the exact 2-point function is defined by a finite set of exponentials. One can obtain the results for the other chirality of correlations by using the middle point reflection $\beta, \gamma \to \gamma, \beta$.

References

[1] J. A. G. Roberts and C. J. Tompson, *Dynamics of the classical heisenberg spin chain*, Journal of Physics A: Mathematical and General **21**(8), 1769 (1988), doi:10.1088/0305-4470/21/8/013.

[2] L. Kavitha and M. Daniel, *Integrability and soliton in a classical one-dimensional site-dependent biquadratic heisenberg spin chain and the effect of nonlinear inhomogeneity*, Journal of Physics A: Mathematical and General **36**(42), 10471 (2003), doi:10.1088/0305-4470/36/42/005.

[3] O. Ragnisco and F. Zullo, *Continuous and discrete (classical) heisenberg spin chain revised*, Symmetry Integrability and Geometry-methods and Applications **3**, 033 (2006).

[4] S. J. Orfanidis, *Su(n) heisenberg spin chain*, Physics Letters A **75**(4), 304 (1980), doi:https://doi.org/10.1016/0375-9601(80)90571-X.

[5] a. Richter, D. Schubert and R. Steinigeweg, *Decay of spin-spin correlations in disordered quantum and classical spin chains*, Phys. Rev. Res. **2**, 013130 (2020), doi:10.1103/PhysRevResearch.2.013130.

[6] M. H. LEE, *Ergodic condition and magnetic models*, International Journal of Modern Physics B **21**(13n14), 2546 (2007), doi:10.1142/S0217979207043877, `https://doi.org/10.1142/S0217979207043877`.

[7] *Time correlation functions and ergodic properties in the alternating xy-chain*, Physica A: Statistical Mechanics and its Applications **89**(2).

[8] F. Borgonovi, G. L. Celardo, M. Maianti and E. Pedersoli, *Broken ergodicity in classically chaotic spin systems*, Journal of Statistical Physics **116**(5), 1435 (2004).

[9] J. V. S. Cannell, J. M. Ortiz de Zárate, *Hydrodynamic Fluctuations in Fluids and Fluid Mixtures*, vol. 30, doi:10.1007/s10765-008-0517-7 (2009).

[10] A. Das, K. Damle, A. Dhar, D. A. Huse, M. Kulkarni, C. B. Mendl and H. Spohn, *Nonlinear fluctuating hydrodynamics for the classical xxz spin chain*, Journal of Statistical Physics **180**(1), 238 (2020).

[11] H. Spohn, *Nonlinear fluctuating hydrodynamics for anharmonic chains*, Journal of Statistical Physics **154**(5), 1191 (2014).

[12] H. Spohn, *Fluctuating hydrodynamics approach to equilibrium time correlations for anharmonic chains*, arXiv: Statistical Mechanics pp. 107–158 (2015).

[13] C. B. Mendl and H. Spohn, *Dynamic correlators of fermi-pasta-ulam chains and nonlinear fluctuating hydrodynamics*, Phys. Rev. Lett. **111**, 230601 (2013), doi:10.1103/PhysRevLett.111.230601.

[14] D. Schubert, J. Richter, F. Jin, K. Michielsen, H. De Raedt and R. Steinigeweg, *Quantum versus classical dynamics in spin models: Chains, ladders, and square lattices*, Phys. Rev. B **104**, 054415 (2021), doi:10.1103/PhysRevB.104.054415.

[15] Ž. Krajnik and T. Prosen, *Kardar–parisi–zhang physics in integrable rotationally symmetric dynamics on discrete space–time lattice*, Journal of Statistical Physics **179**(1), 110 (2020), doi:10.1007/s10955-020-02523-1.

[16] M. Kardar, G. Parisi and Y.-C. Zhang, *Dynamic scaling of growing interfaces*, Phys. Rev. Lett. **56**, 889 (1986), doi:10.1103/PhysRevLett.56.889.

[17] M. Kulkarni and A. Lamacraft, *Finite-temperature dynamical structure factor of the one-dimensional bose gas: From the gross-pitaevskii equation to the kardar-parisi-zhang universality class of dynamical critical phenomena*, Phys. Rev. A **88**, 021603 (2013), doi:10.1103/PhysRevA.88.021603.

[18] A. Das, M. Kulkarni, H. Spohn and A. Dhar, *Kardar-parisi-zhang scaling for an integrable lattice landau-lifshitz spin chain*, Phys. Rev. E **100**, 042116 (2019), doi:10.1103/PhysRevE.100.042116.

[19] P. Kos, B. Bertini and T. c. v. Prosen, *Correlations in perturbed dual-unitary circuits: Efficient path-integral formula*, Phys. Rev. X **11**, 011022 (2021), doi:10.1103/PhysRevX.11.011022.

[20] P. W. Claeys and A. Lamacraft, *Maximum velocity quantum circuits*, Phys. Rev. Res. **2**, 033032 (2020), doi:10.1103/PhysRevResearch.2.033032.

[21] P. W. Claeys and A. Lamacraft, *Ergodic and nonergodic dual-unitary quantum circuits with arbitrary local hilbert space dimension*, Phys. Rev. Lett. **126**, 100603 (2021), doi:10.1103/PhysRevLett.126.100603.

[22] B. Bertini, P. Kos and T. c. v. Prosen, *Exact spectral form factor in a minimal model of many-body quantum chaos*, Phys. Rev. Lett. **121**, 264101 (2018), doi:10.1103/PhysRevLett.121.264101.

[23] B. Bertini, P. Kos and T. Prosen, *Random Matrix Spectral Form Factor of Dual-Unitary Quantum Circuits*, Commun. Math. Phys. **387**(1), 597 (2021), doi:10.1007/s00220-021-04139-2, 2012.12254.

[24] B. Bertini, P. Kos and T. Prosen, *Operator Entanglement in Local Quantum Circuits I: Chaotic Dual-Unitary Circuits*, SciPost Phys. **8**, 067 (2020), doi:10.21468/SciPostPhys.8.4.067.

[25] S. A. Rather, S. Aravinda and A. Lakshminarayan, *Creating ensembles of dual unitary and maximally entangling quantum evolutions*, Phys. Rev. Lett. **125**, 070501 (2020), doi:10.1103/PhysRevLett.125.070501.

[26] J. D. Meiss, *Symplectic maps, variational principles, and transport*, Rev. Mod. Phys. **64**, 795 (1992), doi:10.1103/RevModPhys.64.795.

[27] J. Ding and A. Zhou, *Statistical Properties of Deterministic Systems*, Springer Berlin Heidelberg, doi:10.1007/978-3-540-85367-1 (2009).

[28] B. Bertini and L. Piroli, *Scrambling in random unitary circuits: Exact results*, Phys. Rev. B **102**, 064305 (2020), doi:10.1103/PhysRevB.102.064305.

[29] L. Piroli, B. Bertini, J. I. Cirac and T. c. v. Prosen, *Exact dynamics in dual-unitary quantum circuits*, Phys. Rev. B **101**, 094304 (2020), doi:10.1103/PhysRevB.101.094304.

[30] B. Bertini, P. Kos and T. Prosen, *Exact Correlation Functions for Dual-Unitary Lattice Models in 1+1 Dimensions*, Phys. Rev. Lett. **123**(21), 210601 (2019), doi:10.1103/PhysRevLett.123.210601, 1904.02140.

[31] M. Borsi and B. Pozsgay, *Construction and the ergodicity properties of dual unitary quantum circuits*, Phys. Rev. B **106**(1), 014302 (2022), doi:10.1103/PhysRevB.106.014302, 2201.07768.

[32] M. Gromov, *Pseudo holomorphic curves in symplectic manifolds*, Inventiones mathematicae **82**(2), 307 (1985), doi:10.1007/BF01388806.

[33] D. A. Varshalovich, A. N. Moskalev and V. K. Khersonskii, *Quantum Theory of Angular Momentum*, WORLD SCIENTIFIC, doi:10.1142/0270 (1988).

[34] J. Weber, F. Haake, P. A. Braun, C. Manderfeld and P. Seba, *Resonances of the frobenius-perron operator for a hamiltonian map with a mixed phase space*, Journal of Physics A: Mathematical and General **34**(36), 7195 (2001), doi:10.1088/0305-4470/34/36/306.